Reactivity of $[Cp^*RhPtCl_6]$ ($Cp^* = \eta^5$-C_5Me_5). Synthesis and structures of $[(Cp^*Rh)_2(\mu\text{-}Cl)_3][PtCl_5(CH_3CONH_2)]$ and $[(Cp^*Rh)_2(\mu\text{-}Cl)_3]_2[PtCl_6]$

Keisuke Umakoshi, Katsuo Murata, Shinsuke Yamashita**
Department of Chemistry, Naruto University of Education, Naruto, Tokushima 772 (Japan)
and Kiyoshi Isobe
Institute for Molecular Science, Myodaiji, Okazaki 444 (Japan)

(Received July 15, 1991)

Abstract

Pentamethylcyclopentadienylrhodium dication, $[Cp^*Rh(AN)_3]^{2+}$ (AN = acetonitrile), reacts with hydrogen hexachloroplatinate(IV), H_2PtCl_6, in acetonitrile to give quantitatively, $[Cp^*RhPtCl_6]$ (**1**). The reaction of **1** with $[Cp^*Rh(AN)_3]^{2+}$ in acetonitrile provides $[(Cp^*Rh)_2(\mu\text{-}Cl)_3][PtCl_5(CH_3CONH_2)]$ (**2**). Recrystallization of **1** from hot water gives a different salt, $[(Cp^*Rh)_2(\mu\text{-}Cl)_3]_2[PtCl_6]$ (**3**). Single-crystal X-ray diffraction analyses have revealed that **2** and **3** are salts of the tri-μ-chloro dirhodium cation and pentachloroplatinate with acetamide or hexachloroplatinate. The acetamide molecule in **2** takes an iminol configuration and coordinates to the platinum atom through the nitrogen atom. Crystal data: $[(Cp^*Rh)_2(\mu\text{-}Cl)_3][PtCl_5(CH_3CONH_2)]\cdot 2CHCl_3$, monoclinic, space group $P2_1/n$, $a = 27.456(2)$, $b = 13.131(1)$, $c = 11.706(1)$ Å, $\beta = 91.27(1)°$, $Z = 4$; $[(Cp^*Rh)_2(\mu\text{-}Cl)_3]_2[PtCl_6]$, monoclinic, space group $C2/m$, $a = 27.068(3)$, $b = 11.104(1)$, $c = 8.968(2)$ Å, $\beta = 101.15(2)°$, $Z = 2$.

Introduction

Bimetallic complexes, especially those containing widely divergent transition metal centers, are of interest because of the possibility of emergence of new reactivity patterns which are substantially different from those of bimetallic complexes containing identical or closely related metals [1]. Early–late heterobimetallic complexes form a class of such category. Although there are various examples of early–late heterobimetallic complexes as reviewed by Stephan, both metal centers are mostly organometallic groups. A different class, on the other hand, will emerge by constructing bimetallic complexes with both organometallic and so-called Werner type metal centers.

A wide variety of organometallic compounds that contain the pentamethylcyclopentadienyl (Cp*) ligand have been studied by Maitlis *et al.* [2, 3]. For the following reasons Cp*Rh is one of the suitable organometallic groups for building bimetallic complexes: (i) Rh^{III} shows catalytic behavior in a variety of hydrocarbon transformation, (ii) Cp* itself is less reactive toward nucleophilic attack at the ring carbon atoms, (iii) Cp* highly stabilizes the M–Cp* bond. As the Cp*Rh group has three vacant sites for bonding to other atoms, octahedral metal ion is suitable for forming the face-sharing dinuclear complexes with appropriate bridging ligands. One such candidate is $[PtCl_6]^{2-}$. If it is possible to combine the Cp*Rh group with $[PtCl_6]^{2-}$ in a molecule, each metal ion would be expected to show new reactivity patterns in a cooperative fashion.

In this paper, we describe the synthesis and reactivity of $[Cp^*RhPtCl_6]$ which contains the organometallic group and so-called Werner type metal centers in the molecule, and we also report here the X-ray structure of $[(Cp^*Rh)_2(\mu\text{-}Cl)_3][PtCl_5(CH_3CONH_2)]\cdot 2CHCl_3$ and $[(Cp^*Rh)_2(\mu\text{-}Cl)_3]_2[PtCl_6]$ which were obtained by the reaction of $[Cp^*RhPtCl_6]$ with $[Cp^*Rh(AN)_3]^{2+}$ and by heating $[Cp^*RhPtCl_6]$ in water, respectively.

Experimental

Chemicals

Silver hexafluorophosphate and acetonitrile-d_3 were purchased from Aldrich. Hydrogen hexachloroplatinate(IV) hydrate was thoroughly dried over phosphorus pentoxide *in vacuo*. Pentamethylcyclopentadienylrhodium chloride dimer,

**Author to whom correspondence should be addressed.

0020-1693/91/$3.50

$[Cp^*RhCl_2]_2$, was prepared from rhodium(III) chloride trihydrate (Wako) and 1,2,3,4,5-pentamethylcyclopentadiene (Aldrich) by the literature method [4]. Acetonitrile was distilled over calcium chloride under an argon atmosphere.

Preparation of the complexes

$[Cp^*RhPtCl_6]$ (1)

Method A. To an acetonitrile suspension of $[Cp^*RhCl_2]_2$ (314 mg, 0.5 mmol per 20 cm^3) was added an acetonitrile solution of $AgPF_6$ (506 mg, 2.0 mmol per 10 cm^3) with stirring under an argon atmosphere. A yellow $[Cp^*Rh(AN)_3]^{2+}$ solution [5] was obtained by filtration of AgCl. The yellow solution was added to an acetonitrile solution of H_2PtCl_6 (410 mg, 1.0 mmol per 10 cm^3). A yellow solid which appeared on stirring the solution for 20 min at 20 °C was collected, washed with acetonitrile and ether, and then dried *in vacuo*. At this stage the formation of $[Cp^*RhPtCl_6]$ has not been completed, since the IR spectrum of the yellow solid indicates the existence of an acetonitrile molecule. It was then heated in methanol in order to remove the acetonitrile molecule. The obtained orange solid was washed with methanol and dried *in vacuo*. Yield 550 mg (85%). Anal. Found: C, 18.75; H, 2.39; Cl, 32.9; Pt, 29.2; Rh, 15.4. Calc. for $C_{10}H_{15}Cl_6PtRh$: C, 18.59; H, 2.35; Cl, 32.93; Pt, 30.2; Rh, 15.9%. IR spectrum (Nujol): 1421m, 1162w, 1078m, 1009s, 722m, 588w, 461m, 355s, 319s, 298s cm^{-1}.

Method B. To an acetic acid solution of H_2PtCl_6 (410 mg, 1.0 mmol per 20 cm^3) was added an acetic acid solution of $[Cp^*RhCl_2]_2$ (314 mg, 0.5 mmol per 30 cm^3) with stirring. Stirring was continued for 15 min at 75 °C. The red–brown solution turned to an orange suspension. An orange precipitate was collected, washed with dichloromethane to remove unreacted $[Cp^*RhCl_2]_2$ and with ether, and then dried *in vacuo*; yield 588 mg (91%).

$[(Cp^*Rh)_2(\mu\text{-}Cl)_3][PtCl_5(CH_3CONH_2)]$ (2)

To an acetonitrile suspension of **1** (323 mg, 0.5 mmol per 10 cm^3) was added an acetonitrile solution of $[Cp^*Rh(AN)_3]^{2+}$ (20 cm^3) prepared in the same way as mentioned above ($[Cp^*RhCl_2]_2$ (0.25 mmol); $AgPF_6$ (1.0 mmol)). The mixture was refluxed for 12 h under an oxygen atmosphere. The orange solution was filtered and evaporated under vacuum. The resulting orange residue was extracted with chloroform (50 cm^3). The chloroform solution was evaporated slowly in air. Orange crystals were collected, washed with a small amount of chloroform, and dried *in vacuo*. Yield 101 mg (20%). Anal. Found: C, 27.08; H, 3.65; N, 1.33. Calc. for $C_{22}H_{35}Cl_8NOPtRh_2$: C, 26.06; H, 3.49; N, 1.38%. ^1H NMR (CD_3CN): δ 1.62 (s, 30H, C_5Me_5), 2.35 (s, 3H, CH_3), 7.68 (s and d, 1H, NH, J(Pt–H) = 120 Hz), 10.62 (s, 1H, OH). IR spectrum (Nujol): 3314w, 1639s, 1539w, 1426m, 1335m, 1206s, 1165w, 1081m, 1014s, 918w, 760w, 720w, 588w, 516w, 463m, 455m, 344s cm^{-1}.

$[(Cp^*Rh)_2(\mu\text{-}Cl)_3]_2[PtCl_6]$ (3)

1 (161 mg, 0.25 mmol) was dissolved in hot water (50 cm^3) and the aqueous solution was evaporated slowly in air. Orange plate crystals were collected, washed with water and dried *in vacuo*. Yield 76 mg (77%). Anal. Found: C, 30.26; H, 3.95. Calc. for $C_{40}H_{60}Cl_{12}PtRh_4$: C, 30.54; H, 3.85%. IR spectrum (Nujol): 1164w, 1078m, 1017s, 956w, 719m, 589m, 539w, 463m, 330s cm^{-1}.

X-ray crystal structure analyses

Crystallographic data are summarized in Table 1, along with data collection and refinement information. Intensities were measured on the diffractometer using graphite-monochromated Mo Kα radiation at an ambient temperature of 23 ± 2 °C. Unit cell dimensions were determined by using 36 2θ values for **2**·2$CHCl_3$ and 50 for **3** measured on the diffractometer. The intensity data were corrected for Lorentz and polarization factors and for absorption [6, 7].

The crystal structures were solved by the Patterson–Fourier method. The positional and thermal parameters were refined anisotropically for all non-hydrogen atoms by the block-diagonal-matrix least-squares method. The function minimized was $\Sigma w(|F_o| - |F_c|)^2$, where $w^{-1} = \sigma^2(|F_o|)$ for complex **2**·2$CHCl_3$ and $w^{-1} = \sigma^2(|F_o|) + (0.015|F_o|)^2$ for **3**. The convergence was attained with the R and R_w given in Table 1. No correction was made for secondary extinction. No attempt was made to locate hydrogen atoms in the structure analysis. The atomic scattering factors, with correction for anomalous dispersion of Pt^0, Rh^0 and Cl^0 were taken from ref. 8. Computational work was carried out by using ORTEP [9], RADIEL [7] and standard programs in UNICS III [10].

Measurements

The ^1H NMR spectrum was obtained at 400 MHz with a JEOL GX-400 spectrometer. IR spectra were recorded on a Hitachi 270-50 IR spectrophotometer.

Results and discussion

Preparation, characterization and reaction of $[Cp^*RhPtCl_6]$

The reaction of $[Cp^*Rh(AN)_3]^{2+}$ with H_2PtCl_6 in acetonitrile at room temperature almost quantita-

TABLE 1. Crystallographic data for $[(Cp^*Rh)_2(\mu\text{-}Cl)_3][PtCl_5(CH_3CONH_2)]\cdot 2CHCl_3$ (**2**·$2CHCl_3$) and $[(Cp^*Rh)_2(\mu\text{-}Cl)_3]_2[PtCl_6]$ (**3**)

	2·$2CHCl_3$	**3**
Formula	$C_{24}H_{37}Cl_{14}NOPtRh_2$	$C_{40}H_{60}Cl_{12}PtRh_4$
Formula weight	1252.82	1573.12
Crystal system	monoclinic	monoclinic
a (Å)	27.456(2)	27.068(3)
b (Å)	13.131(1)	11.104(1)
c (Å)	11.706(1)	8.968(2)
β (°)	91.27(1)	101.15(2)
V (Å^3)	4219.0(6)	2644.3(6)
Space group	$P2_1/n$	$C2/m$
Z	4	2
D_{calc} (g cm^{-3})	1.94	1.98
μ(Mo Kα) (cm^{-1})	50.23	45.10
Crystal		
Color and shape	orange rhombic	orange rhombic
Dimensions (mm)	0.51×0.26×0.12	0.06×0.20×0.34
Faces	(100)(010)($\bar{1}$01)	(100)(010)(001)
Data collection instrument	Philips PW1100	Rigaku AFC-5
Scan range (°)	1.2+0.4 tan θ	1.2+0.5 tan θ
Scan mode	ω–2θ	ω–2θ
Scan speed (° min^{-1})	2	4
Background estimation at each end of the scan (s)	10	5
2θ Range (°)	$2.0 \leqslant 2\theta \leqslant 45.0$	$2.0 \leqslant 2\theta \leqslant 60.0$
Octants collected	$\pm h$, $+k$, $+l$	$\pm h$, $+k$, $+l$
No. unique reflections	5796	4010
No. observed reflections with $F_o > 3\sigma(F_o)$	2954	3749
Transmission factor	0.2858–0.5612	0.3922–0.7657
$R(F)$	0.0541	0.0319
$R_w(F)$	0.0627	0.0449

tively gives the yellow solid which still contains acetonitrile molecules. The yellow solid turns to orange [Cp*RhPtCl$_6$] by heating in methanol. If the reaction temperature is raised, further reaction proceeds (*vide infra*) and the yield of [Cp*RhPtCl$_6$] decreases. In order to obtain pure [Cp*RhPtCl$_6$], an extremely purified acetonitrile should be used under an argon atmosphere. We found that the reaction of $[Cp^*RhCl_2]_2$ with H_2PtCl_6 in acetic acid at 75 °C also gives [Cp*RhPtCl$_6$] quantitatively in one step.

Results of elemental analyses are fully consistent with the formula of $[(C_{10}H_{15})RhPtCl_6]$. Since the Cp*Rh cation binds potentially three atoms or groups, the most probable structure is $[Cp^*Rh(\mu\text{-}Cl)_3PtCl_3]$. The IR spectrum of [Cp*RhPtCl$_6$] also supports this structure; it shows characteristic bands at 355, 319 and 298 cm^{-1} which are due to the Pt–Cl stretching vibrations. The appearance of $\nu_1(A_{1g})$, $\nu_2(E_g)$ and $\nu_3(T_{1u})$ indicates that the $PtCl_6$ unit is distorted from O_h symmetry to break down the O_h selection rule and strongly suggests the $Rh(\mu\text{-}Cl)_3Pt$ structure [11].

[Cp*RhPtCl$_6$] reacts with $[Cp^*Rh(AN)_3]^{2+}$ in refluxing acetonitrile and successive extraction of the solid from the reaction mixture with chloroform gives $[(Cp^*Rh)_2(\mu\text{-}Cl)_3][PtCl_5(CH_3CONH_2)]$ (**2**). We could not obtain **2** from the reaction without $[Cp^*Rh(AN)_3]^{2+}$ in acetonitrile. The acetamide is presumably formed by the reaction of acetonitrile coordinated to the Pt atom with water molecule from moisture as suggested in the reaction mechanism for the transformation of nitriles into amides by the use of $TiCl_4$ [12].

$[Cp^*Rh(\mu\text{-}Cl)_3PtCl_3]$ has a very low solubility for an organic solvent. It is converted to the ionic compound, $[(Cp^*Rh)_2(\mu\text{-}Cl)_3]_2[PtCl_6]$ (**3**), in hot water. The IR spectrum of **3** shows only one band (ν_3) at 330 cm^{-1} due to the Pt–Cl stretching vibration. The corresponding Pt–Cl stretching vibration in K_2PtCl_6 appears at 347 cm^{-1} under the same conditions. The difference in the frequency can be ascribed to the effect of each cation [13].

It is noteworthy that the $Rh(\mu\text{-}Cl)_3Pt$ core is reactive and the Cp*Rh group prefers to form the $[Rh(\mu\text{-}Cl)_3Rh]$ structure, as seen in the above reactions.

Structure of 2 and 3

The molecular structures of **2** and **3** were established by X-ray structure analyses. Atomic coordi-

nates are listed in Tables 2 and 3. Selected bond lengths and angles are given in Tables 4 and 5. The perspective drawings of the structures of **2**·2$CHCl_3$ and **3** with the atomic numbering systems are presented in Figs. 1 and 2, respectively. As far as we know, **2** and **3** are the first examples, disclosed by single crystal X-ray analyses, of the tri-μ-chloro bridge structure [14], although several di-μ-chloro bridge structures have been established [15, 16]. Both compounds include the same cation but in different cation/anion ratios: **2** is 1:1, **3** is 2:1. These facts indicate that the charge of the counter anions of **2** and **3** is -1 and -2, respectively. The structure of **3** is described before that of **2**, because $[(Cp^*Rh)_2(\mu\text{-}Cl)_3]^+$ in **3** possesses higher symmetry than in **2**.

As mentioned above, **3** comprises two $[(Cp^*Rh)_2(\mu\text{-}Cl)_3]^+$ ions and a $[PtCl_6]^{2-}$ ion. The two $[(Cp^*Rh)_2(\mu\text{-}Cl)_3]^+$ ions are related by a two-

TABLE 2. Fractional coordinates and equivalent isotropic thermal parameters for $[(Cp^*Rh)_2(\mu\text{-}Cl)_3][PtCl_5(CH_3CONH_2)]\cdot 2CHCl_3$ (**2**·2$CHCl_3$)

	x	y	z	B_{eq}
Pt	0.26990(3)	−0.0094(1)	0.1310(1)	3.3
Rh(1)	0.47637(5)	0.1897(1)	0.3124(1)	2.6
Rh(2)	0.57157(5)	0.3124(1)	0.3972(1)	2.6
Cl(1)	0.3468(2)	−0.0014(4)	0.0519(5)	5.5
Cl(2)	0.3054(2)	−0.0229(4)	0.3107(5)	5.1
Cl(3)	0.1936(2)	−0.0215(4)	0.2080(5)	5.2
Cl(4)	0.2349(2)	0.0016(5)	−0.0507(5)	5.9
Cl(5)	0.2679(2)	0.1667(4)	0.1444(5)	5.1
Cl(6)	0.5072(2)	0.3576(3)	0.2562(4)	3.1
Cl(7)	0.5004(2)	0.2505(4)	0.5048(5)	3.6
Cl(8)	0.5633(2)	0.1480(3)	0.3011(4)	3.5
Cl(9)	0.4146(2)	−0.2428(5)	0.0310(6)	6.8
Cl(10)	0.4977(2)	−0.3374(6)	0.1384(7)	8.7
Cl(11)	0.4185(3)	−0.4585(5)	0.0523(8)	10.0
Cl(12)	0.6087(3)	−0.1720(9)	0.2165(9)	14.4
Cl(13)	0.7019(4)	−0.2517(9)	0.253(1)	18.3
Cl(14)	0.6880(5)	−0.058(1)	0.309(1)	17.2
C(1S)	0.4518(8)	−0.350(2)	0.026(2)	5.4
C(2S)	0.671(1)	−0.154(2)	0.204(3)	10
C(1)	0.4096(6)	0.194(1)	0.210(2)	3.3
C(2)	0.4000(6)	0.170(1)	0.330(2)	3.2
C(3)	0.4241(5)	0.079(1)	0.360(1)	2.4
C(4)	0.4499(6)	0.042(1)	0.259(2)	3.3
C(5)	0.4423(6)	0.116(1)	0.170(2)	2.7
C(1M)	0.3917(7)	0.286(1)	0.146(2)	4.3
C(2M)	0.3665(7)	0.228(2)	0.410(2)	4.7
C(3M)	0.4209(7)	0.022(1)	0.471(2)	4.4
C(4M)	0.4794(7)	−0.054(1)	0.249(2)	4.0
C(5M)	0.4614(7)	0.111(2)	0.051(2)	4.3
C(6)	0.6082(7)	0.457(1)	0.398(2)	3.5
C(7)	0.5986(6)	0.427(1)	0.514(2)	2.9
C(8)	0.6228(6)	0.330(1)	0.537(2)	3.2
C(9)	0.6478(6)	0.301(1)	0.436(2)	3.1
C(10)	0.6385(6)	0.378(1)	0.349(2)	2.9
C(6M)	0.5903(8)	0.555(1)	0.340(2)	5.0
C(7M)	0.5679(7)	0.485(2)	0.598(2)	4.6
C(8M)	0.6237(7)	0.275(2)	0.649(2)	4.4
C(9M)	0.6794(7)	0.211(1)	0.420(2)	4.7
C(10M)	0.6586(8)	0.383(2)	0.232(2)	5.0
N	0.2702(5)	−0.163(1)	0.129(1)	3.7
C(11)	0.2803(6)	−0.229(2)	0.053(2)	4.2
O	0.2935(6)	−0.194(1)	−0.057(1)	7.8
C(12)	0.2807(7)	−0.342(1)	0.059(2)	4.6

TABLE 3. Fractional coordinates and equivalent isotropic thermal parameters for $[(Cp^*Rh)_2(\mu\text{-}Cl)_3]_2[PtCl_6]$ (**3**)

	x	y	z	B_{eq}
Pt	0	0	0	2.1
Rh(1)	0.24478(2)	0	0.20942(5)	2.1
Rh(2)	0.36533(2)	0	0.31381(5)	2.1
Cl(1)	−0.06042(7)	0	0.1522(2)	4.1
Cl(2)	0.04495(5)	0.1463(1)	0.1536(1)	3.8
Cl(3)	0.31236(6)	0	0.0580(2)	2.8
Cl(4)	0.30202(4)	−0.1434(1)	0.3652(1)	3.1
C(1)	0.1739(2)	0	0.2795(8)	2.9
C(2)	0.1774(2)	−0.1042(4)	0.1886(5)	2.8
C(3)	0.1836(1)	−0.0654(4)	0.0420(5)	2.6
C(4)	0.1658(3)	0	0.4424(8)	4.2
C(5)	0.1749(2)	−0.2335(5)	0.2371(6)	3.8
C(6)	0.1877(2)	−0.1427(5)	−0.0922(6)	3.8
C(7)	0.4269(2)	0	0.4985(7)	3.5
C(8)	0.4304(2)	−0.1057(4)	0.4093(5)	3.0
C(9)	0.4338(2)	−0.0663(4)	0.2588(5)	2.9
C(10)	0.4237(3)	0	0.6683(9)	5.8
C(11)	0.4294(2)	−0.2336(5)	0.4576(7)	4.7
C(12)	0.4379(2)	−0.1428(5)	0.1247(6)	4.1

TABLE 4. Selected bond distances (Å) and angles (°) for $[(Cp^*Rh)_2(\mu\text{-}Cl)_3][PtCl_5(CH_3CONH_2)]\cdot 2CHCl_3$ (**2**·2$CHCl_3$)

Pt–Cl(1)	2.326(5)	Rh(1)–C(1)	2.17(2)
Pt–Cl(2)	2.305(6)	Rh(1)–C(2)	2.13(2)
Pt–Cl(3)	2.303(5)	Rh(1)–C(3)	2.13(2)
Pt–Cl(4)	2.319(6)	Rh(1)–C(4)	2.15(2)
Pt–Cl(5)	2.319(5)	Rh(1)–C(5)	2.12(2)
Pt–N	2.02(2)	Rh(2)–C(6)	2.15(2)
Rh(1)···Rh(2)	3.209(2)	Rh(2)–C(7)	2.15(2)
Rh(1)–Cl(6)	2.457(5)	Rh(2)–C(8)	2.15(2)
Rh(1)–Cl(7)	2.467(6)	Rh(2)–C(9)	2.14(2)
Rh(1)–Cl(8)	2.454(5)	Rh(2)–C(10)	2.12(2)
Rh(2)–Cl(6)	2.465(5)	N–C(11)	1.27(3)
Rh(2)–Cl(7)	2.485(5)	C(11)–O	1.43(3)
Rh(2)–Cl(8)	2.443(5)	C(11)–C(12)	1.49(3)
Cl(1)–Pt–Cl(3)	178.6(2)	Cl(6)–Rh(1)–Cl(8)	81.1(2)
Cl(2)–Pt–Cl(4)	179.0(2)	Cl(7)–Rh(1)–Cl(8)	83.2(2)
Cl(5)–Pt–N	176.6(4)	Cl(6)–Rh(2)–Cl(7)	81.8(2)
Pt–N–C(11)	134(1)	Cl(6)–Rh(2)–Cl(8)	81.2(2)
N–C(11)–O	119(2)	Cl(7)–Rh(2)–Cl(8)	83.0(2)
N–C(11)–C(12)	130(2)	Rh(1)–Cl(6)–Rh(2)	81.4(1)
O–C(11)–C(12)	111(2)	Rh(1)–C(7)–Rh(2)	80.8(2)
Cl(6)–Rh(1)–Cl(7)	82.4(2)	Rh(1)–Cl(8)–Rh(2)	81.9(1)

TABLE 5. Selected bond distances (Å) and angles (°) for $[(Cp^*Rh)_2(\mu\text{-}Cl)_3]_2[PtCl_6]$ (3)

Pt–Cl(1)	2.324(2)	Rh(1)–C(1)	2.132(7)
Pt–Cl(2)	2.317(1)	Rh(1)–C(2)	2.137(5)
Rh(1)···Rh(2)	3.216(1)	Rh(1)–C(3)	2.136(4)
Rh(1)–Cl(3)	2.480(2)	Rh(2)–C(7)	2.111(7)
Rh(1)–Cl(4)	2.460(1)	Rh(2)–C(8)	2.151(5)
Rh(2)–Cl(3)	2.459(2)	Rh(2)–C(9)	2.140(5)
Rh(2)–Cl(4)	2.448(1)		
Cl(1)–Pt–Cl(2)	89.94(6)	Rh(1)–Cl(3)–Rh(2)	81.26(5)
Cl(3)–Rh(1)–Cl(4)	81.99(5)	Rh(1)–Cl(4)–Rh(2)	81.88(4)
Cl(3)–Rh(2)–Cl(4)	82.68(5)		

fold axis. The Rh(1), Rh(2), Cl(3), C(1), C(4), C(7) and C(10) atoms lie on a mirror plane, and the rest of the atoms is related to the other half by the mirror plane. The two Cp* rings are approximately parallel and take an eclipsed conformation; the eclipsed conformation is also seen in the structures of $[(Cp^*M)_2(\mu\text{-}OH)_3]^+$ (M = Rh, Ir) [17], while $[Cp^*RhX(\mu\text{-}X)]_2$ (X = Cl, Br) has a staggered conformation [15, 16]. These facts seem to indicate that the tri-μ-halogeno or the tri-μ-hydroxo bridge structure prefers the eclipsed conformation and the di-μ-halogeno bridge structure prefers the staggered one. The Rh···Rh distance (3.216(1) Å) is *c.* 0.5 Å shorter than that of $[Cp^*RhCl(\mu\text{-}Cl)]_2$ (3.7191(6) Å) [15]. The Rh–Cl distances (2.448(1)–2.480(2) Å) are comparable to the corresponding $Rh\text{–}Cl_{bridge}$ distances of $[Cp^*RhCl(\mu\text{-}Cl)]_2$ (2.4649(11), 2.4522(10) Å) but *c.* 0.06 Å longer than the $Rh\text{–}Cl_{terminal}$ distance of the same compound (2.3967(11) Å). The mean Cl–Rh–Cl and Rh–Cl–Rh angles are 82.34 and 81.57°, respectively. The former is comparable to the corresponding angle of $[Cp^*RhCl(\mu\text{-}Cl)]_2$ (81.71(3)°), while the latter is *c.* 16.7° less than the corresponding one (98.29(3)°).

The Pt atom in $[PtCl_6]^{2-}$ lies on the two-fold axis and the mirror plane. The Cl(1) atom also lies on the mirror plane and the Cl(2) atom is related to the other Cl atom by the mirror plane, and these three Cl atoms are further related to the other half by the two-fold axis. The structure of $[PtCl_6]^{2-}$ is identical with that of $K_2[PtCl_6]$ [18]; the Pt–Cl distances of 2.324(2) and 2.317(1) Å and the Cl–Pt–Cl angle between adjacent Cl atoms of 89.94(6)° are almost the same as those in $K_2[PtCl_6]$ (2.314(1) Å and 90°).

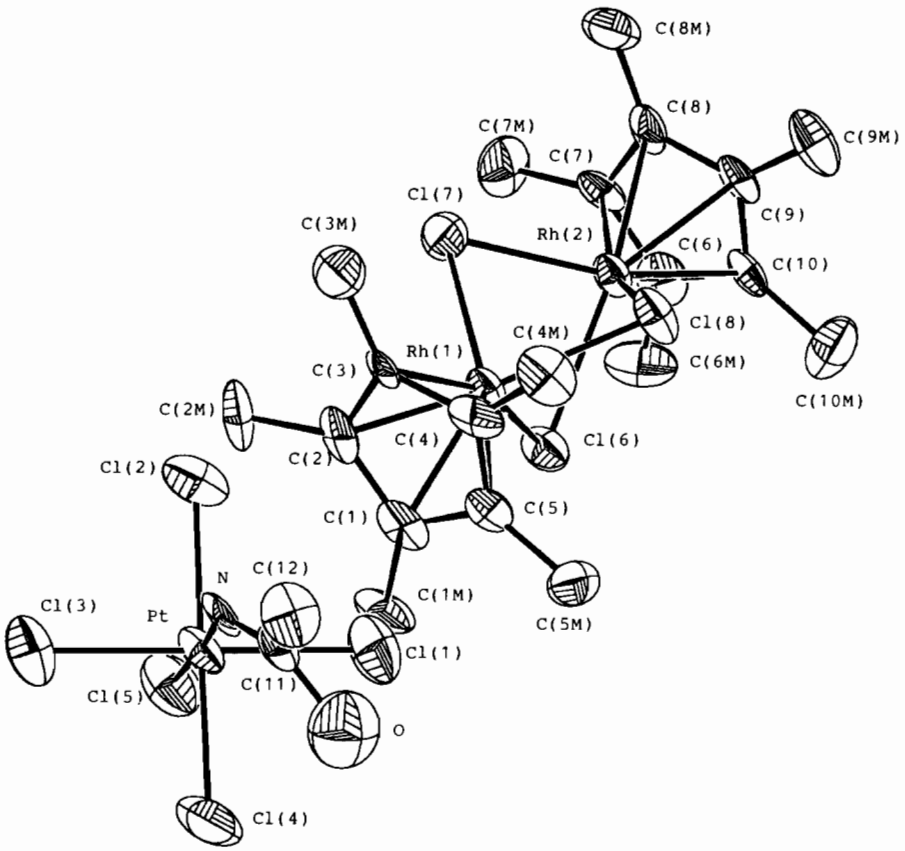

Fig. 1. ORTEP diagram of $[(Cp^*Rh)_2(\mu\text{-}Cl)_3][PtCl_5(CH_3CONH_2)]$ (50% probability contours for all atoms).

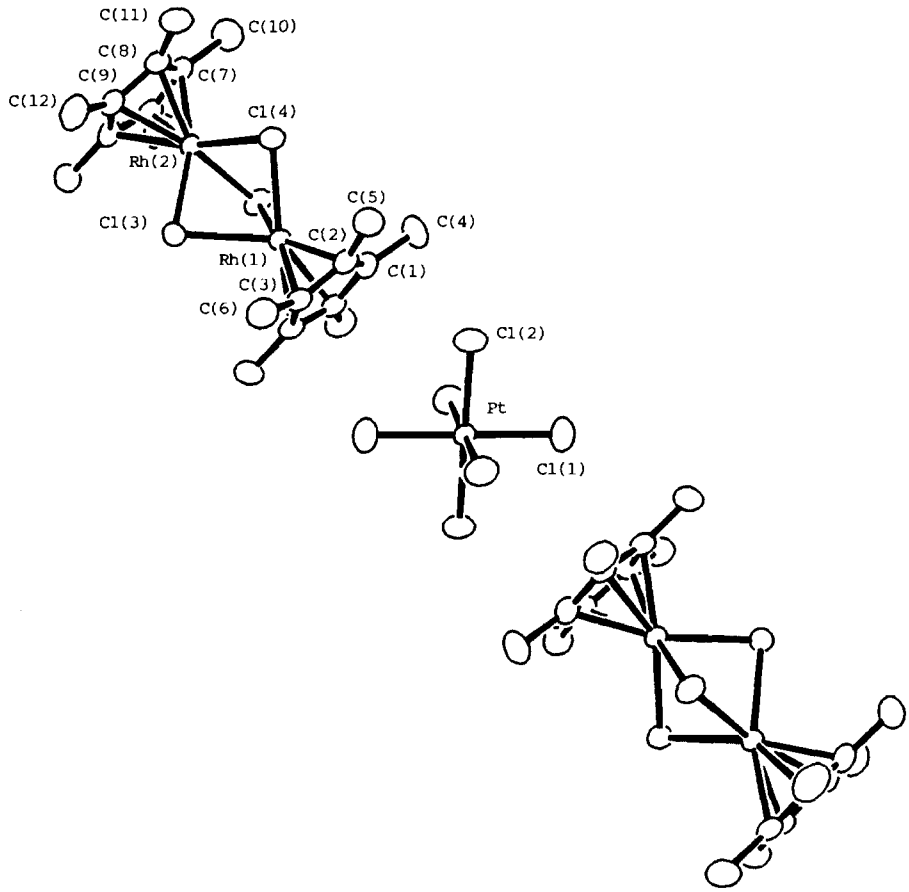

Fig. 2. ORTEP diagram of $[(Cp^*Rh)_2(\mu\text{-}Cl)_3]_2[PtCl_6]$. Thermal ellipsoids are drawn at the 50% probability level.

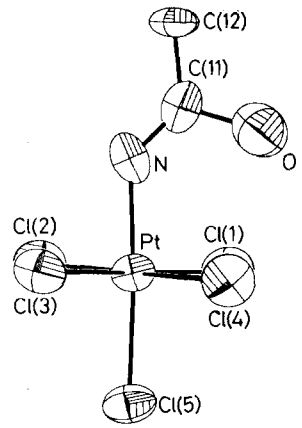

Fig. 3. The structure of $[PtCl_5(CH_3CONH_2)]^-$; details are the same as in Fig. 1.

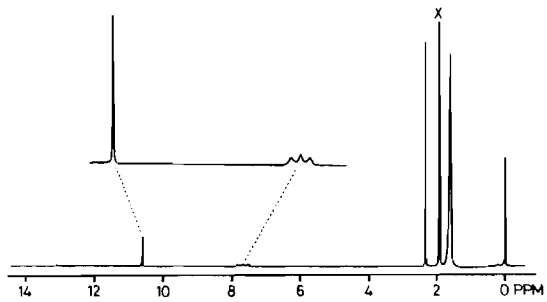

Fig. 4. The 400-MHz ^1H NMR spectrum of $[(Cp^*Rh)_2(\mu\text{-}Cl)_3][PtCl_5(CH_3CONH_2)]$ in CD_3CN solution. X denotes the peak of the solvent.

On the other hand, **2** comprises a $[(Cp^*Rh)_2(\mu\text{-}Cl)_3]^+$ ion and a $[PtCl_5(CH_3CONH_2)]^-$ ion. Although the symmetry of the $[(Cp^*Rh)_2(\mu\text{-}Cl)_3]^+$ ion of **2** is lower than that of **3**, its structural features are identical with those of **3**. The structure of the $[PtCl_5(CH_3CONH_2)]$ anion of **2** is shown in Fig. 3.

The central Pt atom has an octahedral coordination of five Cl atoms and an acetamide ligand. The Pt atom lies in the general position, thus the five Cl atoms are independent. The mean value of the Pt–Cl distances (2.314 Å) is almost the same as in **3** and in $K_2[PtCl_6]$. The Pt–N, C–C, C–O and C–N distances are very similar to the corresponding distances in $[PtCl_2((CH_3)_3CCONH_2)_2]$ which has an iminol configuration: 2.02(2), 1.49(3), 1.43(3) and 1.27(3) Å

for **2**, [2.12(4), 2.05(3)], [1.55(7), 1.53(6)], [1.35(9), 1.40(5)] and [1.20(7), 1.26(5)] Å for $[PtCl_2((CH_3)_3CCONH_2)_2]$, respectively [19]. The acetamide ligand is planar and the C(11) atom has an sp^2 configuration. The IR spectrum of **2** shows the characteristic bands at 3314, 2994 and 1639 cm^{-1} which are due to the N–H stretching vibration, the O–H stretching vibration and the C=N stretching vibration, respectively. These data support that the acetamide ligand coordinates to the Pt atom through the N atom in an iminol configuration.

The NMR spectrum of **2** is shown in Fig. 4. The signals from the acetamide ligand appear at 2.35, 7.68 and 10.62 ppm with 3:1:1 in the intensity ratio, and they are easily assigned to the CH_3 protons, the NH proton and the OH proton, respectively. Interestingly, the coupling of ^{195}Pt with the NH proton was observed in **2** in spite of the rather broad signal of the NH group. The signal pattern of **2** is quite similar to that of $[PtCl_2((CH_3)_3CCONH_2)_2]$ [19] which also has an iminol configuration in $CDCl_3$. From these data we can conclude that the acetamide ligand in complex **2** takes an iminol configuration and coordinates to the Pt atom through the N atom in both solid and solution.

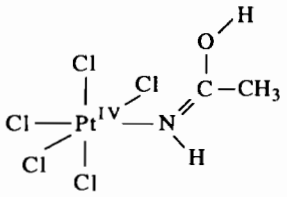

Supplementary material

Listings of thermal parameters (Tables SIA and SIB), full lists of bond lengths and bond angles (Tables SIIA and SIIB), and tables of calculated and observed structure factors are available from the authors on request.

Acknowledgements

This work was supported by a Grant-in-Aid for Scientific Research (No. 02740303 and No. 03740317) from the Ministry of Education, Science, and Culture of Japan and was partly supported by the Joint Studies Program (1990–1991) of the Institute for Molecular Science.

References

1 D. W. Stephan, *Coord. Chem. Rev., 95* (1989) 41.
2 P. M. Maitlis, *Chem. Soc. Rev., 10* (1981) 1.
3 P. M. Maitlis, I. M. Saez, N. J. Meanwell, K. Isobe, A. Nutton, A. Vázquez de Miguel, D. W. Bruce, S. Okeya, P. M. Bailey, D. G. Andrews, P. R. Ashton and I. R. Johnstone, *New J. Chem., 13* (1989) 419.
4 Y. Hayashi, Y. Ozawa and K. Isobe, *Inorg. Chem., 30* (1991) 1025.
5 C. White, S. J. Thompson and P. M. Maitlis, *J. Chem. Soc., Dalton Trans.,* (1977) 1654.
6 L. K. Templeton and D. H. Templeton, *Abstr., American Crystallographic Association Proc.,* Ser. 2, Vol. 1, American Crystallographic Association, Storrs, CT, 1973.
7 P. Coppens, T. N. Guru Row, P. Leung, E. D. Stevens, P. J. Becker and Y. W. Yang, *Acta Crystallogr., Sect. A, 35* (1979) 63.
8 *International Tables for X-ray Crystallography,* Vol. IV, Kynoch Press, Birmingham, UK, 1974.
9 C. K. Johnson, *ORTEP II, Rep. ORNL-5138,* Oak Ridge National Laboratory, Oak Ridge, TN, 1976.
10 T. Sakurai and K. Kobayashi, *Rikagaku Kenkyuusho Hokoku (Rep. Inst. Phys. Chem. Res.), 55* (1979) 69.
11 K. Nakamoto, *Infrared and Raman Spectra of Inorganic and Coordination Compounds,* Wiley–Interscience, New York, 4th edn., 1986, p. 154.
12 T. Mukaiyama, K. Kamio, S. Kobayashi and H. Takei, *Chem. Lett.,* (1973) 357.
13 D. M. Adams and S. J. Payne, *J. Chem. Soc., Dalton Trans.,* (1975) 215.
14 J. W. Kang and P. M. Maitlis, *J. Organomet. Chem., 30* (1971) 127.
15 M. R. Churchill, S. A. Julis and F. J. Rotella, *Inorg. Chem., 16* (1977) 1137.
16 M. R. Churchill and S. A. Julis, *Inorg. Chem., 17* (1978) 3011.
17 A. Nutton, P. M. Bailey and P. M. Maitlis, *J. Chem. Soc., Dalton Trans.,* (1981) 1997.
18 S. Ohba and Y. Saito, *Acta Crystallogr., Sect. C, 40* (1984) 1639.
19 D. B. Brown, R. D. Burbank and M. B. Robin, *J. Am. Chem. Soc., 91* (1969) 2895.